Evaluation of Smartphone-based Indoor Positioning Using Different Bayes Filters

Petra Hafner, Thomas Moder, Manfred Wieser
Institute of Navigation
Graz University of Technology
Graz, Austria
{petra.hafner, thomas.moder, manfred.wieser}@tugraz.at

Thomas Bernoulli
Institute for Building Informatics
Graz University of Technology
Graz, Austria
thomas.bernoulli@tugraz.at

***Abstract*—Within the research project LOBSTER, a system for analyzing the behavior of escaping groups of people in crisis situations within public buildings to support first responders is developed. The smartphone-based indoor localization of the escaping persons is performed by using positioning techniques like WLAN fingerprinting and dead reckoning realized with MEMS-IMU. Hereby, WLAN fingerprinting is analyzed especially in areas of few access points and the IMU-based dead reckoning is accomplished using step detection and heading estimation. The data of all sensors are fused in combination with building layouts using different Bayes filters. The behavior of the Bayes filters is investigated especially within indoor environments. The restrictions of the Kalman filter are shown as well as the advantages of a Particle filter using building plans.**

Keywords - Bayes filters, pedestrian navigation, smartphone sensors, first responder, MEMS-IMU

I. INTRODUCTION

The focus of the project LOBSTER is the development of a localization and monitoring system which investigates the escape behavior of people in crisis situations within public buildings (e.g., hospitals, shopping centers, airports, universities, etc.). The information about the escape way and the activity of the affected persons is used to support first responders.

The localization as well as the activity recognition (walking, standing) of the escaping persons is realized by the positioning technologies GNSS, WLAN and Inertial Measurement Units (IMU) of common smartphones. In case of distress, the determined positions are transmitted to the Location-Based Service (LBS) center, where the monitoring of the casualties and the coordination of the rescue units take place. In this center, these data are used in combination with building layouts and mathematical filter technologies (Particle filter and Kalman filter) to estimate the persons' positions and their predicted escape ways. This information supports the first responders in establishing a significantly improved coordination and resource scheduling of the rescue teams. The first responders are equipped with a device which is used on the one hand for the communication with the LBS center to get all the necessary information about the casualties and on the other hand to perform a self-localization in case of a rescue operation, see Fig. 1. The positions of the first responders are simultaneously visualized on their mobile devices and in the LBS center to facilitate the central coordination of the rescue operation.

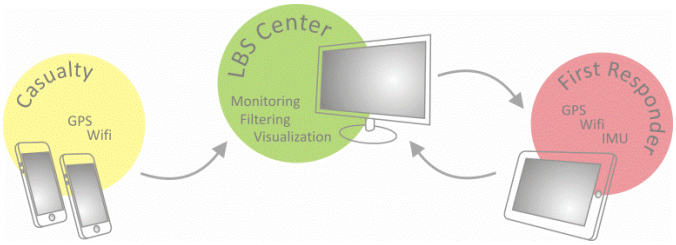

Figure 1. The LBS center of the project LOBSTER monitors the casualties by evaluating their position and activity data and assists the first responders by transmitting the operation-essential data.

First responders represent rescue forces from several units like fire fighters or rescue units and are equipped with specially tailored mobile devices. These mobile devices enable multi-sensor positioning based on GNSS, WLAN and IMU measurement data. For the coordination concept within LOBSTER, a two-way communication with the LBS center is necessary. For the support of the first responders in action, the mobile device visualizes the track of the first responder and the escaping groups of people as overlay to maps and building layouts of the operation area.

The localization of the casualties is based on common smartphones. The reason is that a representative amount of persons has to be tracked to draw conclusions on the escape behavior of people in public buildings. Statistics predict, that in three to five years more than 50 % of all people in Europe will own a smartphone, which may be representative for all persons involved in a specific scenario. Smartphones do comprise various sensors for position determination and communication. Within LOBSTER, a smartphone application is developed which observes measurement signals of position and communication sensors (GNSS and WLAN) as well as of the IMU without interrupting the ordinary use of the phone. In case of an emergency, the application uses the observations to perform an anonymous localization and sends the positioning information to the LBS center.

Since the measurement data of all sensors are evaluated independently on the smartphone (GNSS single point

positioning, WLAN fingerprinting, IMU-based dead reckoning), an integration process is carried out in the LBS center to utilize the performance of a multi-sensor system.

For this application, two different position filters, the Kalman filter and the Particle filter which are most common in the field of navigation, are implemented and investigated. Both filters belong to the family of Bayes filters which recursively estimate the posterior probability of the state space conditioned on the data collected so far.

In case of the Kalman filter, the posterior probability is approximated by the first and second moments, i.e., mean and covariance. This filter approach is optimal for linear Gaussian systems. The Particle filter is a sample-based approach, where the posterior probability is represented by sets of samples.

The advantage of this filter is that the samples (particles) can represent arbitrary probability densities. Compared to a general grid-based approach, this filter has the ability to focus the particles on regions in the state space with a high probability. Since the estimation within the Particle filter is based on samples, a building layout can be integrated by defining conditions to samples in non-probable areas. Consequently, additional information can be extracted and integrated within the filtering process.

The focus of the paper is set on the smartphone-based indoor localization of the casualties using the WLAN and IMU data. Since it cannot be expected, that every public building is equipped with lots of WLAN access points, the key aspect are the investigations based on the availability of a few access points. Consequently, the paper is organized as follows: First, the independently performing positioning algorithms WLAN fingerprinting and IMU-based pedestrian dead reckoning are shown, starting with investigations of the measurement data, describing the implemented algorithms and analyzing the results. In addition, the building layouts used in the filtering process are explained. The estimated position, heading and step information together with the building layouts are then integrated within two different Bayes filters – the Kalman filter and the Particle filter. The performance of both filters is compared and analyzed using different positioning scenarios (reduction of the available WLAN access points).

II. SMARTPHONES

A. Application of smartphones within LOBSTER

The smartphone is the latest step in the mobile phone evolution and first appeared in 2007. Nowadays, it is the most ubiquitous technical device present in the industrial world due to its properties mobility and connectivity.

Today, about 75 % of people in Germany are using a mobile phone. In 2012, more than 50 % of owned mobile phones were smartphones. It is estimated, that by 2017 mainly smartphones will be sold as mobile phones [1]. Every third person overall owns a smartphone nowadays, with rising tendency. In 2012, more smartphones than mobile phones were sold in Germany [2].

Due to these facts, the distribution of smartphones among population is today more than 30 % and will rise up to 70 % in three to four years from now. This is and will be a representative group of people to extrapolate from people with smartphones to all people in general, especially for situations like the assistance of first responders. Although the smartphone distribution among different groups of age and income is diverse, it cannot be extrapolated linearly.

B. Smartphone Sensors

Since the appearance of the first smartphone six years ago, the evolution of the smartphone as a positioning sensor has made amazing progress. Sensors like GPS, WLAN transceiver, accelerometers and cameras were present from the very beginning. This emerged to sensor arrays including GPS, WLAN, accelerometers, magnetometers, gyroscopes, barometers, temperature sensors, proximity sensors and cameras.

The smartphone sensors used for the work presented in this paper are the WLAN sensor and the IMU composed of accelerometers gyroscopes and magnetometers. These sensors are fabricated as Micro-Electrical-Mechanical-Systems (MEMS) today. MEMS describe an electronic technology as a development of the electrical integrated circuits which are present in electronics for over 50 years. Applying the MEMS technology, sensors can be produced in very small sizes. However, such sensors experience strong bias errors, temperature as well as turn-on variations. According to [3], inertial MEMS sensors are one of the most interesting developments in the last 30 years.

The smartphone used within the work presented in this paper is the Samsung Galaxy Nexus. All of the following raw sensor data, measurements as well as training data were recorded with the built-in sensors of this roughly two year old smartphone exemplarily. Hereafter, first the sensor sampling followed by the raw data analysis of the smartphone sensors is presented.

1) Sensor sampling

Sensor sampling is obviously not the most important task for a mobile phone. Therefore, no continuous sensor sampling can be expected. However, it is possible to set an approximate sampling rate, but it will not be continuous and blunders in the sampling are present. Depending on the used smartphone, a sampling frequency of the inertial data of up to 100 Hz can be realized. In Fig. 2 the sampling data of one accelerometer axis is shown exemplarily.

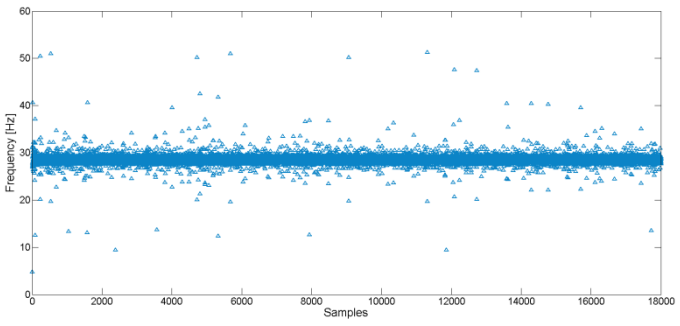

Figure 2. Accelerometer sensor sampling of a smartphone

978-1-4673-1954-6/12/$31.00 ©2012 IEEE

2) WLAN

In the following figures, raw WLAN measurements observed with a smartphone are shown. The data is acquired using a WLAN Router Linksys E2500 which is dual-band capable. The WLAN router is set up to work with 2.472 GHz as well as 5.240 GHz. The smartphone sampling rate for WLAN measurements was set to 1 Hz.

The WLAN raw data in static conditions is shown in Fig. 3. The WLAN measurements of the smartphone are given as received signal strength (RSS) in dB referring to the signal of 1 mW, often noted as dBm. A measurement noise of 1.2 dB for the 2.472 GHz and 0.6 dB for the 5.240 GHz frequency is visible in the static data. Especially some blunders in the 2.472 GHz band are visible. Therefore, filtering of the raw RSS data is necessary for the WLAN positioning based on RSS measurements.

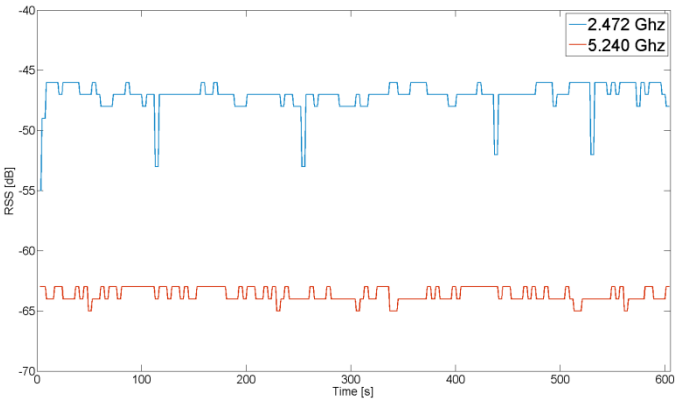

Figure 3. Static RSS measurement of a smartphone

The theoretical path loss according to [11] can be given by

$$PL_{(d)} = PL_{(d_0)} + 10 \cdot n \cdot log_{10}(\frac{d}{d_0}), \qquad (1)$$

where $PL_{(d_0)}$ is measured at $d_0 = 5m$ distance and received from the mean RSS over 10 minutes, see Fig. 3. The value n is defined according to [4] with $n = 2$ in free space, or $2 < n < 6$ for office buildings. In Fig. 4, the theoretical path loss in free space is compared to the actual WLAN measurements every meter on a defined (free space) proving track for 30 m.

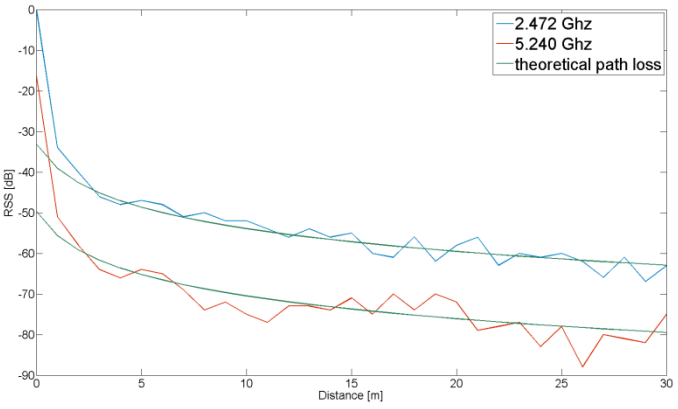

Figure 4. RSS measurement of a smartphone with varying distance

A measurement noise of 2 to 3 dB compared to the theoretical path loss can be observed on the 30 m proving track.

The raw accelerometer, gyroscope and magnetometer data are not explicitly shown in this paper. However, significant higher noise and sensor variations of the inertial smartphone sensors compared to low-cost consumer-grade inertial units, otherwise used in inertial navigation, are present.

3) Sensor biases

MEMS sensor errors can be distinguished - bias, scale factor, non-linearity, hysteresis and noise are present. However the bias error due to turn-on and temperature variations is the biggest error.

Accelerometer bias errors can be estimated by accomplishing turn-over maneuvers, shown in Fig. 5. The bias error within this analysis is in the range of up to 0.4 m/s².

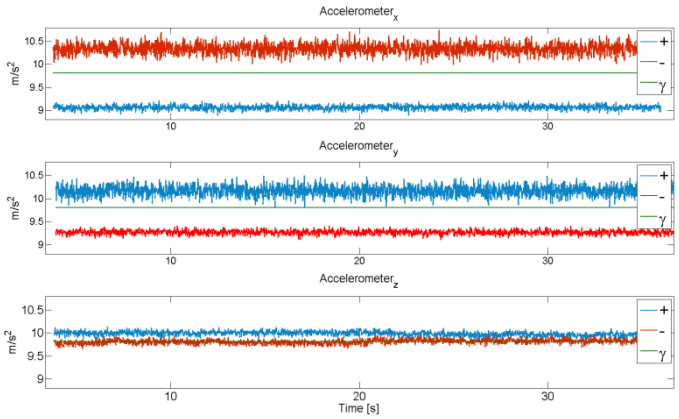

Figure 5. Smartphone accelerometer bias error

Gyroscope raw data is highly filtered and the mean value is nearly zero when the sensor is at rest. However, the investigations of the dynamic process show huge gyroscope bias errors up to 0.5 °/s. Integrated, this equates to a heading error of some 10 ° in one minute, if there is no fusion with absolute sensors.

The sensor bias errors for the magnetometer data are not analyzed in detail because the biggest influence in magnetic measurements is the magnetic deviation, see [5]. Magnetic deviation is mainly dependent on the building infrastructure and cannot be estimated. Magnetic distortions are best avoided by performing a magnetometer and gyroscope sensor fusion, adjusted to the expected motion of the sensors.

The experienced sensor biases of the used MEMS sensors are huge for inertial navigation purposes, which is caused by the small size architecture of the MEMS embedded in smartphones. Therefore, the strict sensor integration of the inertial measurements like proposed in [3] are not applicable with smartphone sensors and more rugged and simplified positioning algorithms are applied.

III. BUILDING MODEL FOR PARTICLE FILTERS

As additional information for the position filters, building plans may be used as an analytic sensor. In this section, the creation of the floor plans used as input to the Particle filter is described and some background information presented.

Buildings are three dimensional by their nature. If two dimensional floor plans are created to represent these 3D structures, some information is lost. Therefore, it is state of the art to use 3D models to represent buildings and extract 2D floor plans if necessary for specific applications. If enriched with non-structural information, these building models are called Building Information Models (BIM). There exist many commercial applications for architects and civil engineers to create BIMs. Unfortunately, those applications are complex, expensive, and use proprietary file formats by default. The Industry Foundation Classes (IFC) data model defined by the International Alliance for Interoperability (IAI, now buildingSMART) is an emerging standard supported by many of those applications. As its intent is to describe building and construction industry data, it is very complex too; its advantage is the open specification.

A floor plan used as input to a Particle filter does not have to be very sophisticated: It must be possible to check if a person can traverse on a straight line from a point A to a point B on a given floor. This requirement can already be fulfilled by binary bitmaps using white pixels for allowed areas and black ones for denied areas. Thus, the tool should allow exporting this kind of bitmaps and providing the functionality to import existing floor plans to minimize the work needed. Additionally, it should save georeferencing information of the exported bitmaps facilitating the use in mixed indoor-outdoor scenarios with GNSS position information.

The AIONAV IPS Editor was a perfect match as it has a light-weight BIM, imports DXF files, and allows saving floor plans with user-defined resolution as georeferenced bitmap (PNG file with accompanying world file).

The basic idea of its BIM is to specify the area of a building accessible to humans. This area is defined by a set of simple polygons (the boundary of the polygon does not cross itself) which are connected at specific segments of their outline. Each area has a height attribute allowing the creation of a 3D surface modeling multiple floors of a building. To make it possible to create 2D floor plans, these areas are assigned to floors. To further structure the model, floors are sub-elements of buildings and buildings belong to a region.

To determine the segment(s) of the outline of an area at which it is possible for a person to traverse to another area, connection elements are defined. A connection element consists of at least one pair of references to lines, one line of each involved area. The lines are segments of the outline of the areas and must be geometrically exactly equal. The connection element is placed as sub-element of the first common ancestor of the involved areas. I.e., a connection element connecting two areas on the same floor is a sub-element of this floor and would be sub-element of the region if the connected areas are part of different buildings.

The hierarchical model is then saved as XML-file which allows straight forward parsing, see Tab. 1. The region element does not only contain building sub-elements but also a *coordinateMapping* element which encodes the georeferencing information.

TABLE I. EXCERPT OF A BUILDING MODEL XML FILE

```
<?xml version="1.0" encoding="UTF-8"?>
<region xmlns="http://bauinformatik.tugraz.at/ips-bim-editable" id="1">
 <building id="0" label="Steyrergasse30">
  <floor id="0" label="EG">
   <area height="0.0" id="0">
    <line id="0">
     <point id="0" x="24" y="23"/>
     <point id="1" x="24" y="20"/>
    </line>
    [...]
   </area>
   <area height="0.0" id="37">
    [...]
    <line id="7">
     <point id="0" x="24" y="23"/>
     <point id="1" x="24" y="20"/>
    </line>
    [...]
   </area>
   <connection>
    <pair first="1.0.0.0.0" second="1.0.0.37.7" type="door"/>
   </connection>
  </floor>
 </building>
 <coordinateMapping>[...]</coordinateMapping>
</region>
```

Once the model is defined, each floor can be exported to a georeferenced bitmap. The resolution can be defined by the user as pixel per meter ratio. In Fig. 6, the floor plan exported as bitmap can be seen. Additionally, the test scenario, on which the analysis presented in this paper is conducted, is shown as a trajectory.

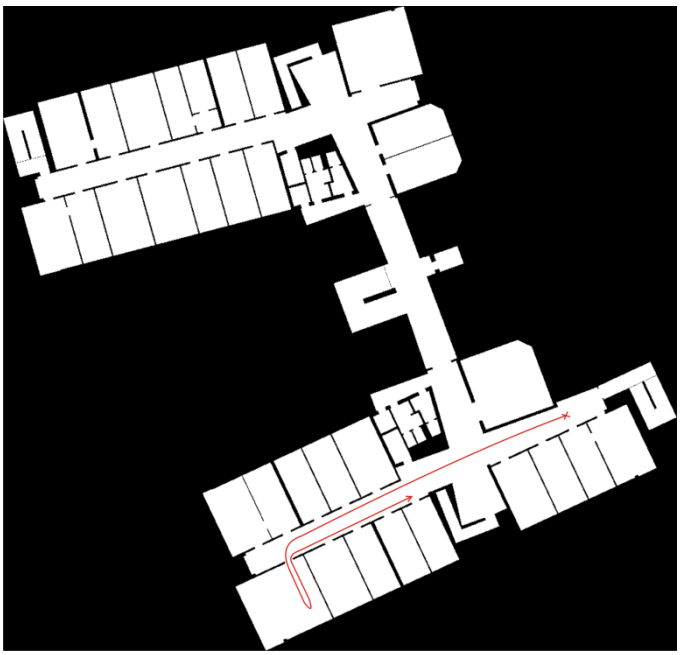

Figure 6. Floor plan exported as binary bitmap with test track

IV. INDOOR POSITIONING WITH SMARTPHONES

Compared to outdoor positioning, indoor positioning is very limited according to the presence and visibility of electrical signals. No ubiquitous system for indoor navigation exists. Possible technologies for indoor positioning could be methods based on Cell-ID, RFID, inertial navigation, image-based navigation, WLAN, magnetic field, ultra-wide band positioning and many more.

From these possibilities, the methods applied to smartphones today are based on WLAN, magnetic field, inertial navigation and visual navigation. Among the absolute position techniques available, WLAN has the most common, already existing infrastructure indoors. Within the project LOBSTER, for the indoor positioning, WLAN positioning and inertial navigation based on step detection and heading estimation have been investigated.

A. *WLAN positioning*

WLAN positioning provides absolute positioning based on measurements of received signal strength (RSS) from different WLAN access points. The main motivation behind WLAN positioning is to use existing infrastructure. Within the work of [14] and [15], WLAN positioning within an artificial environment, where access points were set up just for positioning purposes, is investigated.

In WLAN positioning, proximity-based positioning, trilateration and fingerprinting are the possible methods for positioning. The accuracy of proximity-based positioning is directly correlated to the number of available access points and is therefore not applicable with a low number of access points. Trilateration is conducted with the measured signal strength. Since the signal strength is strongly influenced by the building structure, the whole building would have to be taken into account to gather useful results from trilateration with a few access points. Fingerprinting corresponds to matching a measurement set of RSS data to a predefined set of training data, called the fingerprinting database. For WLAN fingerprinting, neither time-synchronization of the access points is necessary nor their position has to be known.

The mostly used improvement to a plain matching of the best reference point is called K-Nearest Neighbor (KNN) [4]. Here, the K-best fingerprinting reference points are used to calculate the estimated position of the measurement device, where

$$\hat{p}_{KNN} = \sum(p_i,\ _{i=1,K}) \qquad (2)$$

is the most probable position of the measurement point. Best results can be achieved if $3 \leq K \leq 5$.

When analyzing static and kinematic RSS measurements, blunders and measurement noise in the static case can be observed. The RSS noise rises when moving the measurement device. Due to the unstable measurement behavior of the smartphone WLAN sensor, RSS filtering is conducted with a simple Kalman filter based on the raw RSS measurement data with an empirically defined measurement noise. Additionally, the region-based reference point selection proposed in [12] is implemented.

In the following, the WLAN-only positioning based on a KNN fingerprinting with $K = 4$ is shown. A comparison of WLAN processing with all visible access points (more than 15 MAC addresses can be observed within the testing ground) on the test track and positioning just with the use of three access points is analyzed. In Fig. 7, the fingerprinting of the test track processed with all visible access points is shown.

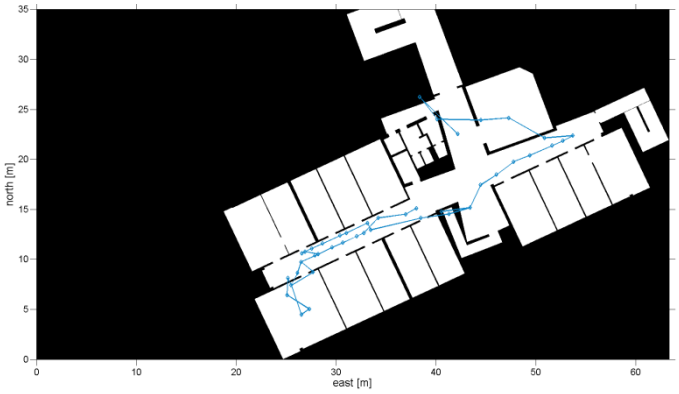

Figure 7. WLAN fingerprinting with all available access points

In Fig. 8 the fingerprinting processed with just three distinct access points for the same track is visualized.

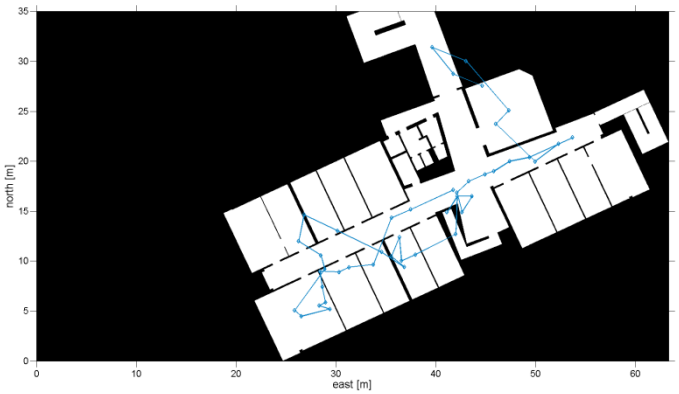

Figure 8. WLAN fingerprinting with three distinct access points

When comparing the two results of Fig. 7 and Fig. 8, it is obvious that the trajectory processed with all available access points is more accurate compared to the reference trajectory in Fig. 6. In both cases, the fingerprinting needs some seconds for the RSS Kalman filter to smooth the raw measurements and produce stable results. Afterwards, the trajectory processed with all available access points features at least room-level accuracy. Contrary to that, the trajectory processed with just three access points is not able to produce room level accuracy within the defined setup.

B. *Dead Reckoning*

Applying Pedestrian Dead Reckoning (PDR) algorithms on measurements of mobile devices, the sensor position relative to the user is a crucial factor. [9] proposes a tree classifier for identifying the actual position of the mobile device similar to activity recognition. For the PDR algorithm, the sensor position and orientation at the beginning has either to be fixed and known or to be initialized. Within this paper, a fixed sensor

position of the smartphone relative to the user is assumed. The smartphone is hand-held in walking direction during the presented measurements, which is the assumed position when a pedestrian is navigating with his smartphone. The PDR positioning is partitioned into a step detection and the estimation of the step heading.

1) Step detection

For step detection, multiple methods exist, see [8] for a comparison of step length estimators as well as [9] with a step frequency approach and [10] with an event detection. Simple step detection is more robust than step length or step duration estimation with hand held smartphone sensors, due to the given sensor noise and bias error behavior.

In the following, the step detection with smartphone accelerometer measurements is presented in Fig. 9. A step event is created every time at the end of a detected step. A step is detected if an upward motion is followed by a downward motion for a defined timespan. An up- or downward motion is just considered if the total acceleration is above or beneath an empirically defined boarder. That is, why actions not similar to steps are not recognized.

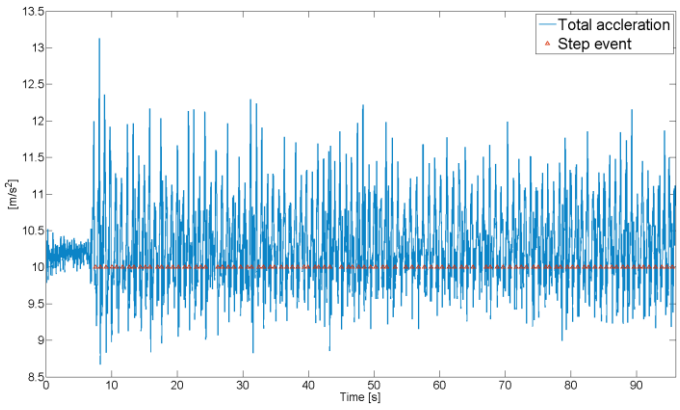

Figure 9. Step detection with accelerometer measurements

The distance finally calculated out of the step event se is given by $d = se \cdot K$, where K is an empirically defined constant for a specific user. With this fixed step length algorithm, a mean distance misclosure of 2 m for different walking speeds can be observed within a proving track of 30 m. Although the step detection is adopted for a defined sensor position, the misclosure is caused by different walking speeds.

2) Heading estimation

For the estimation of a step heading, the magnetic orientation of the smartphone is filtered with the angular rate in local level up-direction. Therefore, the magnetic heading computation and a transformation of the measured angular rates have to be performed. Since the smartphone is hand-held in walking direction and assumed to be in a constant orientation, the difference between heading and yaw is neglected.

In order to compute a magnetic orientation out of a three axes magnetometer, the leveling angles roll and pitch have to be known. The attitude angles roll r and pitch p are computed by leveling. A leveling is conducted with the measurements of the accelerometer in three axes a_x, a_y, and a_z and is given in [7] by

$$p = \tan^{-1}\left(\frac{-a_x}{\sqrt{a_y^2+a_z^2}}\right) \quad (3)$$

$$r = \tan^{-1}\left(\frac{-a_y^2}{-a_z^2}\right) \quad (4)$$

The magnetic yaw computed with the magnetometer in three axes and the known attitude angles roll and pitch is given in [7] by

$$y_{mag} = \tan^{-1}\left(\frac{-a_z\, cos(r)+a_z\, sin(p)}{a_x\, cos(p)+a_y\, sin(p)\, sin(r)+a_z\, sin(p)\, cos(r)}\right) \quad (5)$$

For gaining the angular rate of yaw in a local level frame, a transformation of the gyroscope measurements in three axes has to be applied. If the rotation matrix R_l^b is given with its rotations about roll, pitch and yaw by $R_l^b = R_1(r)R_2(p)R_3(y)$, the angular rate vector in up-direction referring to a local-level system is then given by

$$\omega_l = R_b^l \omega, \quad (6)$$

where ω contains the gyroscope measures g_x, g_y and g_z and ω_l contains the time-derivations $\dot{r}$, $\dot{p}$ and $\dot{y}$ in the chosen local level frame. If just the angular rate of yaw is desired, the yaw angle is not needed for the creation of R_b^l.

The computed relative $\dot{y}$ and absolute y_{mag} can then be filtered to gain heading information based on the magnetometer heading and the angular rates in up-direction. Such a heading is more robust to magnetic disturbances, see Fig. 10. It is seen, that small variations in the magnetic field can be overcome through integrating and filtering the angular rate.

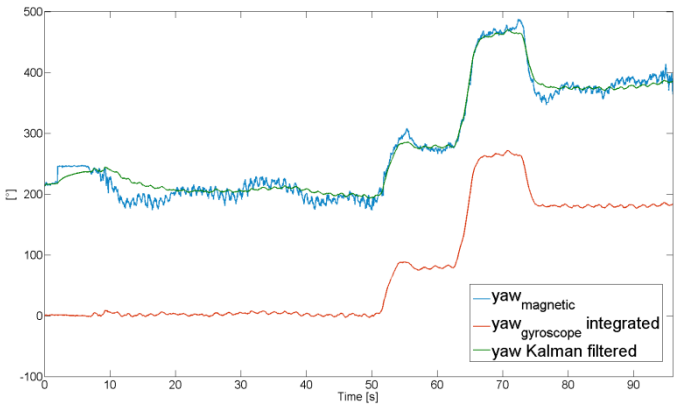

Figure 10: Heading estimation with filtering of smartphone data

The use of gyroscope-only data is another reasonable approach which was investigated. However, such an approach only works when either the device orientation is known or a calibration of the device orientation respectively to the user motion is applied. Such a device orientation can be determined out of heading information with absolute position solutions such as GNSS or WLAN positioning. However, neither GNSS nor state-of-the-art WLAN positioning provides a position accuracy which is accurate enough that the computation of an absolute heading is reasonable.

V. BAYES FILTER

Within the project LOBSTER, two different filtering approaches belonging to the family of Bayes filters – the Kalman filter and the Particle filter - are investigated. The principle of Bayesian filtering is constituted by two models and enables the estimation of the state of a dynamic system [16], [19]. The system model describes the propagation of the state with time, while the measurement model is based on the functional dependency between the noisy measurements and the actual state. The evolution of the state (prediction step) is defined by

$$x_k = f_k(x_{k-1}, v_{k-1}), \quad (7)$$

with x_k and x_{k-1} representing the states at epoch k and $k-1$, and v_{k-1} being the process noise. The measurement model

$$z_k = h_k(x_k, n_k), \quad (8)$$

defining the relationship between the observations z_k, their corresponding covariance n_k and the state x_k, together with the transition model facilitates a recursive estimation of the actual state x_k. In case of the Bayesian approach, these two models are expressed in a probabilistic form. A posterior probability density function (PDF) of the state based on all available information is determined.

Within the prediction stage, the prior PDF of the state at epoch k is determined via the Chapman-Kolmogorov equation

$$p(x_k|z_{1:k-1}) = \int p(x_k|x_{k-1})p(x_{k-1}|z_{1:k-1})dx_{k-1}, \quad (9)$$

with the assumption that

$$p(x_k|x_{k-1}, z_{1:k-1}) = p(x_k|x_{k-1}) \quad (10)$$

is a Markov chain of first order. While the PDF of the state transition $p(x_k|x_{k-1})$ can be expressed by the system model and the process noise, the PDF of the measurement update is dependent on the likelihood function $p(z_k|x_k)$ which is influenced by the measurement model and the measurement noise n_k

$$p(x_k|z_k) = \frac{p(z_k|x_k)p(x_k|z_{1:k-1})}{p(z_k|z_{1:k-1})}. \quad (11)$$

In the update step, the posterior density of the state x_k is determined by combining the measurements z_k their measurement noise n_k and the prior density $p(x_k|x_{k-1})$ by applying the Bayes' rule. The Kalman filter and the Particle filter represent the Bayesian filter approach with some restrictions. An optimal solution in general cannot be determined analytically ([16], [18] and [19]).

A. Kalman Filter

The Kalman filter is a parameterized approach of the Bayesian filter where the probability distribution functions of the prediction and the update stage are represented by the first and second moments (mean and covariance) of the probability distributions [17]. The Kalman filter is the optimal filter for tracking applications, if the assumptions hold the system as well as the measurement equations are linear and their corresponding PDFs are Gaussian [5]. Consequently, the posterior probability $p(x_k|z_{1:k})$ is Gaussian, if $p(x_{k-1}|z_{1:k-1})$ is Gaussian and v_{k-1} and n_k are drawn from Gaussian distributions of known parameters. The system and the measurement equation can be expressed as follows

$$x_k = F_k x_{k-1} + v_{k-1} \quad (12)$$
$$z_k = H_k x_k + n_k \quad (13)$$

By replacing the process noise v_{k-1} and the measurement noise n_k by their covariances Q_{k-1} and R_k, the moments of the parameterized form of the Bayes approach can be determined with the equations 14 to 18. The Kalman filter is split into three steps – the prediction, the update and the computation of the Kalman gain. The Kalman gain declares the impact of the actual measurements on the estimation of the actual state.

Prediction step:

$$\hat{x}_{k|k-1} = F_{k-1}\hat{x}_{k-1|k-1} \quad (14)$$
$$P_{k|k-1} = Q_{k-1} + F_{k-1}P_{k-1|k-1}F_{k-1}^T \quad (15)$$

Update step:

$$\hat{x}_{k|k} = \hat{x}_{k|k-1} + K_k(z_k - H_k\hat{x}_{k|k-1}) \quad (16)$$
$$P_{k|k} = (I - K_k H_k)P_{k|k-1} \quad (17)$$

Computation Kalman gain:

$$K_k = P_{k|k-1}H_k^T\left(H_k P_{k|k-1}H_k^T + R_k\right)^{-1} \quad (18)$$

Although the Kalman filter works best in a Gaussian environment and in case of linear system and measurement equations, the performance for indoor application is restricted, since the integration of building layouts causes a modification of the Gaussian distribution.

B. Particle Filter

In case of a Particle filter, the probability distributions defined within the Bayesian approach are represented by a set of particles randomly distributed over the state space and of corresponding weights [16]. The propagation of the particles is regulated by the state transition model. After propagating the particles (prediction step), the particles are weighted corresponding to the probability distribution of the measurement model and the actual measurements. According to these computed weights, the particles are newly-distributed. In the initialization step all particles are randomly distributed over the whole state space (e.g. over a whole building), after the resampling, the distribution of the particles represents the posterior distribution of the state x_k. The higher the number of particles, the more the posterior PDF approaches the functional description of the posterior PDF.

The sequential importance sampling (SIS), where the particles are drawn from an importance weight, is the general framework for the implementation of the Particle filter. The particles are not drawn from the probability$p(x_k|z_{0:k})$, they are distributed according to the weight

$$\omega_k^i \propto \omega_{k-1}^i \frac{p\left(z_k|x_k^i\right)p(x_k^i|x_{k-1})}{q(x_k^i|x_{k-1}^i, z_k)}, \quad (19)$$

with $q\left(x_k^i\middle|x_{0:k-1}^i, z_k\right)$ being the importance probability density function, [16] and [18]. The posterior filtered density function corresponds to

$$p(x_k|z_{1:k}) \approx \sum_{i=1}^{N_s} \omega_k^i \delta(x_k - x_k^i). \quad (20)$$

If N_s approaches infinity, the approximated posterior converges to the true PDF. However, the problem of the SIS approach is the degeneration of the particles, since after a few iterations only some particles of high weights survive. For this case a resampling step has to be considered. Within the paper, the SIR (Sequential Importance Resampling) algorithm has been chosen to keep as many samples as possible with non-zero weights [16], [17]. Beside the SIR algorithm, also other effective resampling approaches exist, see [18] and [20].

In principle, the implemented Particle filter is based on approaches of [17], [21], and [24]. For the integration of building layouts within the Particle filter, different algorithms have been tested, based on [21], [22], [23], and [25].

C. Setup

The estimated local positions of the WLAN fingerprinting, the travelled distance out of the step detection and the estimated heading are used beside the building layout as input for the Bayes filters.

In case of the Kalman filter the building layout is only used for the visualization. The algorithm itself is performed with a common pedestrian motion model for the prediction step, while all available measurement data and their corresponding covariances are used in the update step. The measurement vector has following structure

$$z_k = (x_{WLAN}, y_{WLAN}, \Delta d, \vartheta)^T. \quad (21)$$

In contrast, the prediction step of the Particle filter uses the output of the PDR and the building layout to propagate the particle cloud in the best possible way. Involving the building layout in the prediction step enables an elimination of invalid particles before entering the update step. Another approach would be the integration of the map within the update step by computing an appropriate weight based on the map's probability. However, this approach does not work that effective, which is also shown in [25]. For the computation of the importance weight, the WLAN positions are used.

To compare the performance of both filters, two different measurement scenarios have been chosen. First, all available WLAN access points are applied to determine a trajectory. In a second scenario, the fingerprinting is performed with a fingerprinting data base with only three access points for the whole area.

VI. RESULTS

In the following, the filtering results of the two mentioned scenarios (all access points vs. three access points) are shown.

A. Scenario 1 – all access points

Fig. 11 shows the raw WLAN and PDR trajectories in comparison with the Kalman filtered solution. It is indicated that the Kalman filter process eliminates the drift of the PDR by combining the DR data with the WLAN positioning data. The last room on the left side of the floor can be entered correctly.

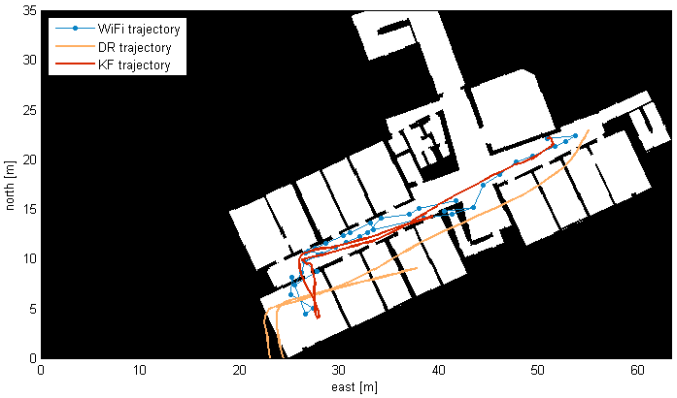

Figure 11. Kalman filtered trajectory based on a WLAN trajectory with all available access points.

The same can be observed in the Particle filtered trajectory in Fig. 12. However, the integration of the building layout affects the result with a marginal smoothing. The visualized grey trajectory corresponds to the weighted mean of the particles. Although the integration of the building layout works very well, in some figures an overlaying of the Particle filtered trajectory with the walls can be seen, since the resulting trajectory is derived by a weighted averaging of the particles.

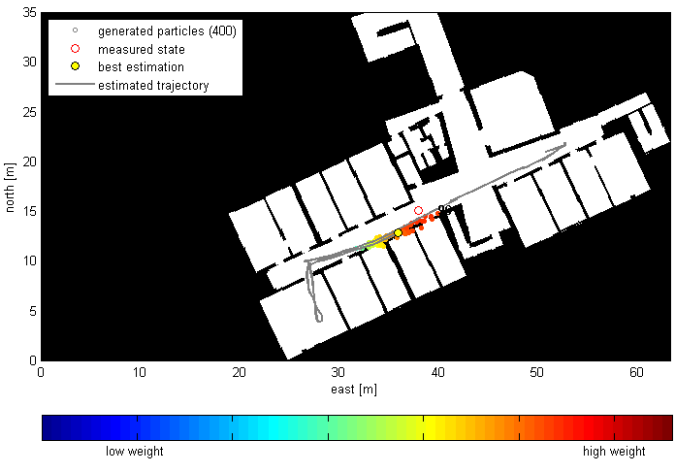

Figure 12. Particle filtered trajectory based on a WLAN trajectory with all available access points.

By performing a fingerprinting with all available access points, nearly no differences can be observed in the Kalman filtered and Particle filtered trajectories.

B. Scenario 2 – three access points

In Scenario 2, the WLAN fingerprinting is based on three access points. Consequently, the determined WLAN trajectory shows a worse performance, see Fig. 13. By applying the Kalman filter, a smoothed trajectory is computed, but the trajectory goes through walls, where a room entering is impossible.

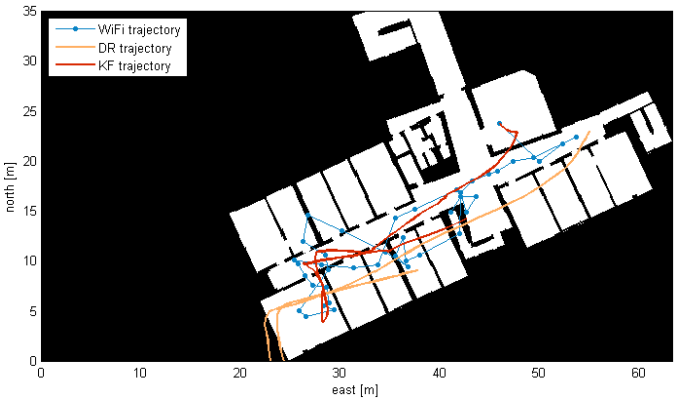

Figure 13. Kalman filtered trajectory based on a WLAN trajectory with three access point.

Comparing the Kalman filtered result with the Particle filter trajectory in Fig. 14, a rigorous improvement can be detected.

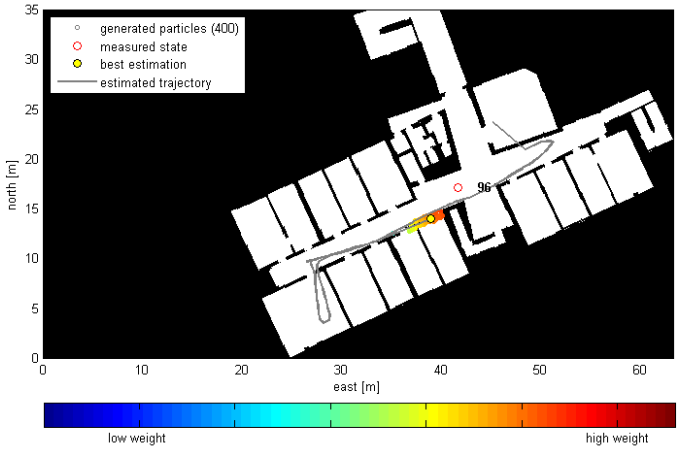

Figure 14. Particle filtered trajectory based on a WLAN trajectory with three access points.

The trajectory does not leave the floor on the way to the last room on the left side of the floor, enters the room correctly and goes back on the right way, see also Fig 15.

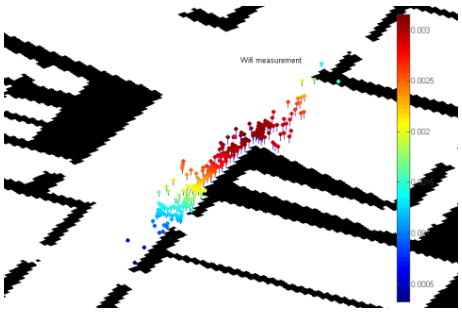

Figure 15. Particles moving along the walls.

Just at the beginning of the trajectory, a large deviation can be seen. The reason for this discrepancy is the first WLAN position, which indicates a large difference to the real trajectory. However, the filter converges quickly to the true trajectory, which can be pointed out with Fig. 16 and Fig. 17.

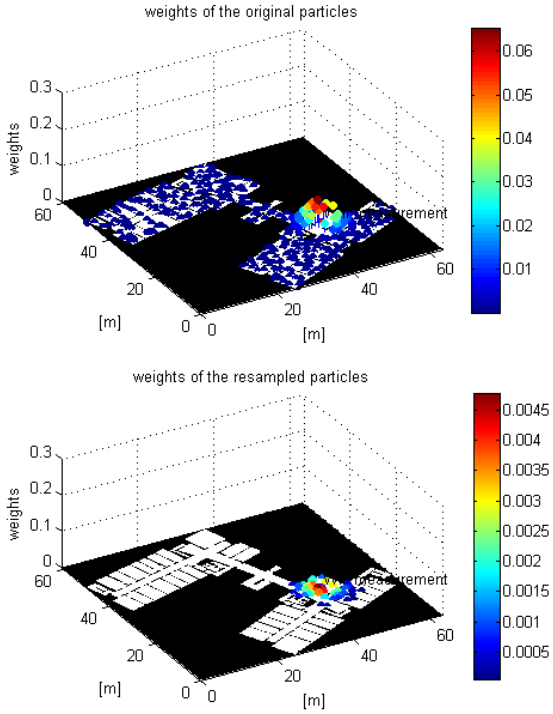

Figure 16. Initialization of the particles and applying the first WLAN measurements within the update step.

In Fig. 16, the initialization of the particles over the whole building is shown. By using the first WLAN measurements in the resampling step, the particles surround the WLAN measurement. The change of the PDF in direction to the true trajectory is realized already after one more epoch (Fig. 17).

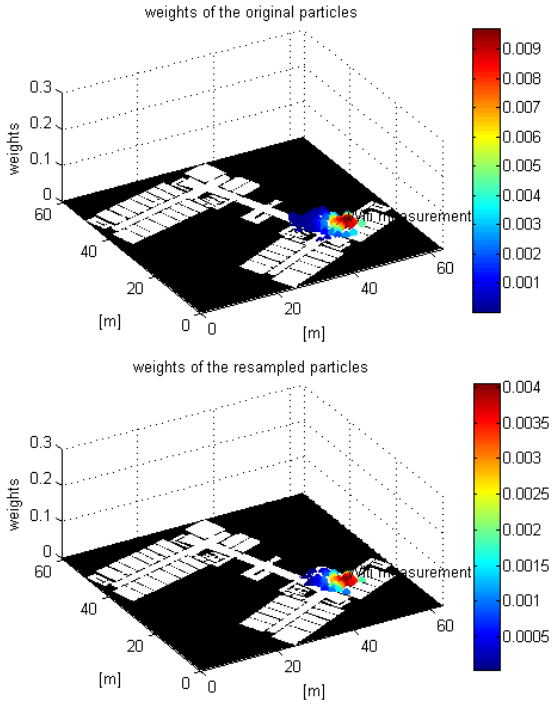

Figure 17. Change of the PDF representation after the second epoch. Despite the bad measurement in the beginning, the filter converges very fast.

VII. CONCLUSION

The investigations show, that the performance of the Particle filter is much better than the one of the Kalman filter in case of a bad WLAN trajectory. The integration of map information enables a correct passing of floors and entering of rooms. Applying the filters on accurate measurement data, leads nearly to the same results.

Finally, it can be concluded, that the use of the Particle filter enables tracking also in environments with few WLAN access points. Since WLAN routers increase their coverage continuously, it is important to be able to consider WLAN positioning with fewer access points, as the access point density will most likely decrease.

ACKNOWLEDGMENT

This work is performed in the frame of the Austrian research promotion program KIRAS, funded by the Federal Ministry for Transport, Innovation and Technology via the Austrian Research Promotion Agency, project number 832335.

REFERENCES

[1] BITKOM, http://www.bitkom.org/files/documents/BITKOM_Presseinfo_Besitz_von_Smartphones_16_04_2012(1).pdf. http://www.bitkom.org/de/presse/74532_71854.aspx, Berlin, 2012.

[2] Statista, smartphones---statista-dossier-2013-1.ppt. http://de.statista.com/statistik/studie/id/3179/dokument/smartphones-statista-dossier-2012/. 2013.

[3] D. H. Titterton, J. L. Weston, Strapdown inertial navigation technology, Second Edition. Progress in Astronautics and Aeronautics, MIT Lincoln Laboratory, Lexington, Masachusetts, 2004.

[4] A. Kushki, K. N. Plataniotis, and A. N. Venetsanopoulos, WLAN Positioning Systems. Principles and Applications in Location-Based Services. Cambridge University Press, Cambridge, 2012.

[5] B. Hofmann-Wellenhof, K. Legat, and M. Wieser, Navigation – Principles of Positioning and Guidance. Springer, Wien, 2003.

[6] A. Bensky, Wireless Positioning. Technologies and Applications. Artech House, Boston, 2008.

[7] P. D. Groves, Principles of GNSS, inertial, and multisensor integrated navigation systems. Artech House, Boston, 2008

[8] D. Alvarez, R. C. Gonzales, A. Lopez, and J. C. Alvarez, Comparison of step length estimators from wearable accelerometer devices: Proceedings of the 28th IEEE EMBS Annual International Conference, New York City, 2006.

[9] V. Renaudin, M. Susi, and G. Lachapelle, Step length estimation using handheld inertial sensors, Sensors – Open Access Journal, Switzerland, 2012.

[10] O. J. Woodman, Pedestrian localization for indoor environments, Dissertation, University of Cambridge, Cambridge, 2010.

[11] R. Dutzler, and M. Ebner, Indoor Navigation by WLAN Location Fingerprinting, unpublished, 2013.

[12] W. Meng, W. Xiao, W. Ni, and L. Xie, Secure and robust Wi-Fi fingerprinting indoor localization, International Conference on Indoor Positioning and Indoor Navigation, Guimaraes, Portugal, 2011.

[13] W. Xiao, W. Nei, and Y. K. Toh, Integrated Wi-Fi fingerprinting and inertial sensing for indoor positioning, International Conference on Indoor Positioning and Indoor Navigation, Guimaraes, Portugal, 2011.

[14] E. Navarro, B. Peuker, and M. Quan, Wi-Fi localization using RSSI fingerprinting. California Polytechnical State University, Computer Engineering Department, California, USA, 2010.

[15] W. Grossmann, M. Schauch, and S. Hakobyan, RSSI based WLAN indoor positioning with personal digital assistants, IEEE International Workshop on Intelligent Data Acquisition and Advanced Computing Systems, Germany, 2007.

[16] B. Ristic, S. Arulampalam, and N. Gordon, Beyond the Kalman Filter – Particle Filters for Tracking Applications. Artech House, Boston, London, 2004.

[17] S. Thrun, W. Burgard, and D. Fox, Probabilist Robotics. The MIT Press, Cambridge, Massachusetts, London, England, 2006.

[18] A. Doucet, N. de Freitas, and N. Gordon, Sequential Monte Carlo Methods in Practice. Springer, New York, 2010.

[19] M.S Arulampalam, S. Maskell, N. Gordon, and T. Clapp, "A tutorial on particle filters for online nonlinear/non-Gaussian Bayesian tracking,", IEEE Transactions on Signal Processing, Vol.50, No.2, Feb.2002.

[20] M. Afonso, "Particle filter and extended Kalman filter for nonlinear estimation: a comparative study", Instituto Superior Técnico (IST), the School of Engineering of the Technical University of Lisbon, 2008.

[21] J. Straub, Pedestrian indoor localization and tracking using a particle filter combined with a learning accessibility map, Bachelor Thesis, Institute for Real-Time Computer Systems, Technische Universität München, 2010.

[22] I. Spassov, M. Bierlaire, and B. Merminod, "Map-matching for pedestrians via Bayesian inference", European Navigation Conference–Global Navigation Satellite Systems, May 2006.

[23] P. Davidson, J. Collin, and J. Takala, "Application of particle filters for indoor positioning using floor plans", Ubiquitous Positioning, Indoor Navigation and Location-Based Service (UPINLBS) 2010. IEEE, Oct. 2010.

[24] F. Gustafsson, F. Gunnarsson, N. Bergman, U. Forssell, J. Jansson, R. Karlsson, and P.-J. Nordlund, "Particle filters for positioning, navigation and tracking", IEEE Transactions on Signal Processing, Vol. 50, No. 2, Feb. 2002.

[25] S. Kaiser, M. Khider, and P. Robertson, "A maps-based angular PDF for navigation systems in indoor and outdoor environments", International Conference on Indoor Positioning and Indoor Navigation (IPIN) 2011, Guimarães, Portugal, Sep. 2011.